Materials Advances

ROYAL SOCIETY OF CHEMISTRY

PAPER

View Article Online
View Journal | View Issue

Check for updates

Cite this: *Mater. Adv.*, 2025, 6, 2328

Nitric oxide-scavenging micelles alleviate airway inflammation in asthma *via* Th2 cytokine modulation†

Daoxiang Rong,[ac] Shanshan Fang,[bc] Shaohu Huo,[a] Paiyu Lin,[a] Jian Cheng,*[d] Jingfang Hong*[b] and Shenggang Ding*[a]

Received 17th November 2024,
Accepted 4th March 2025

DOI: 10.1039/d4ma01135j

rsc.li/materials-advances

Allergic asthma is a chronic inflammatory airway disease. Nitric oxide (NO), a key molecule in this inflammation, is elevated in asthma and contributes to poor control and worsened symptoms. In this study, we developed nitric oxide-scavenging micelles (NOSMs) to reduce NO concentration and alleviate pulmonary inflammation in an allergic mouse model. NOSMs effectively lower airway NO levels, significantly inhibit the production of pro-inflammatory factors IL-6 and IL-13, and promote the release of IFN-γ. Thus, NOSMs may play a key role in treating allergic asthma by scavenging NO and modulating Th2-related pulmonary inflammation.

1. Introduction

Asthma is a chronic inflammatory disease characterized by airway inflammation and remodeling, resulting from the interplay between genetic and environmental factors. It is one of the most prevalent and recurrent chronic diseases, affecting approximately 4.3% of adults globally, which translates to over 300 million individuals.[1–3] Furthermore, industrialization is projected to increase this number to 400 million by 2025.[4] The global prevalence of asthma not only imposes a substantial burden on patients and healthcare systems but also presents significant challenges to clinical management.

Chronic airway inflammation is the hallmark of asthma, complicating disease control. Thus, rapid management of airway inflammation is essential. Asthma treatment primarily relies on medications, particularly inhaled corticosteroids, which reduce inflammatory factors, inhibit the NF-κB and MAPK signaling pathways, suppress inflammatory cells, and alleviate symptoms.[5–7] However, long-term corticosteroid use can lead to drug resistance and various side effects, including osteoporosis, growth suppression in children, and diabetes.[8–13] New therapies, including long-acting β2-agonists, leukotriene receptor antagonists, and monoclonal antibodies, are currently under development.[2,14,15] Thus, rapid management of airway inflammation is essential to underscore the need for more effective treatment strategies.

Nitric oxide (NO) as an endogenous signaling molecule plays a significant role in respiratory diseases such as asthma. In the airway inflammatory response of asthma patients, NO plays a critical role in the inflammatory process. Overproduction of NO can lead to reaction with specific reactive oxygen species (ROS) within biological systems, resulting in the formation of reactive nitrogen species (RNS). These RNS and ROS significantly intensify airway inflammatory responses and promote tissue injury.[16,17] For example, IL-13 plays a crucial role in exacerbating airway inflammation, increasing airway hyperresponsiveness, and promoting airway remodeling in asthma patients.[18–20] Literature research shows that NO promoted the secretion of IL-13. Meanwhile, IL-13 increases the elevation of inducible nitric oxide synthase (iNOS) in epithelial cells, thereby increasing NO levels.[21] On the other hand, high concentrations of NO can promote airway inflammation, leading to airway hyperresponsiveness and structural remodeling through multiple pathways such as NO-cGMP-PKG-TRPVl, NO-cGMP-PKG-MAPK, and NO-cAMP-PKA-CREB.[22–25] Therefore, reducing NO concentration at lesion sites may serve as an effective therapeutic approach for asthma.

Nanoparticles significantly enhance asthma treatment by improving drug bioavailability, reducing dosing frequency, and serving as delivery agents to prevent rapid drug degradation. In recent years, polymer nanoparticles and solid lipid nanoparticles have been extensively investigated for asthma treatment by improving pharmacokinetics, prolongation circulation, reducing drug

[a] *Department of Pediatrics, the First Affiliated Hospital of Anhui Medical University, Hefei, Anhui, 230022, China. E-mail: dingsg@ahmu.edu.cn*
[b] *School of Nursing of Anhui Medical University, Hefei, Anhui, 230022, China. E-mail: hongjingfang@ahmu.edu.cn*
[c] *Department of Pediatrics, the First Affiliated Hospital of Bengbu Medical University, Bengbu, Anhui, 233004, China*
[d] *Suzhou Institute for Advanced Research, University of Science and Technology of China, Suzhou, 215123, China. E-mail: cjivn@ustc.edu.cn*

† Electronic supplementary information (ESI) available. See DOI: https://doi.org/10.1039/d4ma01135j

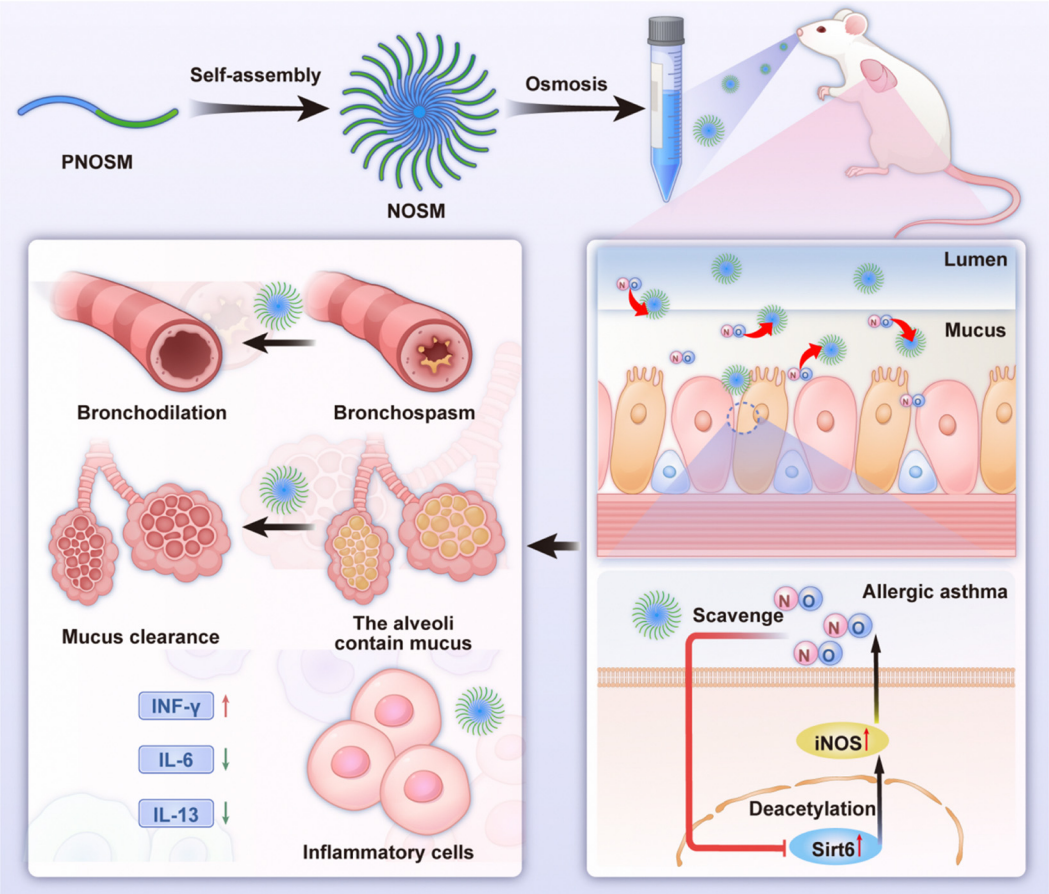

Scheme 1 Fabrication of NO-scavenging micelles (NOSMs) and treatment of allergic asthma mice *via* nebulization. NOSMs inhibit the generation of SIRT6 and subsequently reduce the synthesis of iNOS by absorbing NO. NOSMs effectively clear NO from inflamed areas and suppress the expression of pro-inflammatory factors (IL-6 and IL-13), while increasing the levels of the anti-inflammatory factor (IFN-γ).

toxicity, and targeting drug delivery.[26–29] Among these, polymer nanoparticles are the most widely used drug delivery materials due to their high modifiability and advantages like excellent drug loading capacity and controllable release characteristics. In this study, we developed nitric oxide-scavenging micelles (NOSMs) that effectively scavenge NO through the formation of benzotriazole (BTA) moieties. Herein, we demonstrate that NOSMs significantly reduced the expression of the pro-inflammatory factors IL-6 and IL-13 in LPS-induced macrophages, while increasing the levels of the anti-inflammatory factor IFN-γ, as shown in Scheme 1. Therefore, NOSMs successfully achieve inflammation suppression. To further explore the application of NOSMs in allergic asthma, we established a mouse model induced by ovalbumin (OVA). Therefore, NOSMs significantly alleviated airway inflammation and remodeled the microenvironment, underscoring their potential value in the treatment of allergic asthma.

2. Materials and methods

2.1 Synthesis and characterization of NOSMs

2.1.1 Synthesis of 2-(3-(2-aminophenyl)ureido)ethyl methacrylate hydrochloride (APUMA). The synthetic route and characterization of APUMA are shown in Fig. S1 (ESI†). Typically, *o*-phenylenediamine (2.7 g, 25 mmol) was dissolved in 20 mL anhydrous THF. 2-Isocyanatoethyl methacrylate (3.88 g, 25 mmol) was dissolved in anhydrous THF and added dropwise. The mixture was further stirred at room temperature overnight. After that, THF was removed under reduced pressure and the residue was precipitated into an excess of diethyl ether. The insoluble solid was isolated by filtration, and washed with diethyl ether (4.6 g, 70%). ^{1}H NMR (400 MHz, DMSO-d_6, δ, ppm; Fig. S1, ESI†) δ 7.63 (s, 1H), 7.23 (d, J = 6.4 Hz, 1H), 6.80 (t, J = 7.5 Hz, 1H), 6.69 (d, J = 6.3 Hz, 1H), 6.53 (t, J = 7.5 Hz, 1H), 6.31 (t, J = 5.8 Hz, 1H), 6.09 (s, 1H), 5.70 (s, 1H), 4.71 (s, 2H), 4.13 (t, J = 5.5 Hz, 2H), 3.37 (dd, J = 11.1, 5.4 Hz, 2H), 1.90 (s, 4H).

2.1.2 Synthesis of PNOSM diblock copolymers through RAFT polymerization. APUMA (262 mg, 1.0 mmol), PEG-based macroRAFT agent (114 mg, 0.05 mmol), and AIBN (1.6 mg, 0.01 mmol) were dissolved in 500 μL of DMF. The reaction tube was degassed by three freeze–pump–thaw cycles and then sealed under vacuum. After heating at 60 °C in an oil bath for 10 h, the reaction was quenched into liquid nitrogen and opened, and the mixture was precipitated into diethyl ether/DCM (4 : 1, v/v) three times. The sediment was filtered and dried under vacuum overnight. The degree of polymerization (DP) of the PNOSM diblock

was determined to be 15 based on the ^{1}H NMR analysis (Fig. S2, ESI†). The number average molecular weight (M_n) was 6.3 kDa, and the molecular weight distribution (M_w/M_n) was determined to be 1.2.

2.1.3 Fabrication and titration of NOSMs. Typically, the PNOSM diblock copolymer (1 mg) was dissolved in 1 mL of THF : DMF = 1 : 1 (v/v), which was then quickly injected into 9 mL of DI water in one shot. The mixture was stirred at room temperature for 5 min. After that, the resulting dispersion was transferred into a dialysis tube (MWCO = 14 kDa) and was dialyzed against DI water for 12 h to remove the organic solvent. Fresh deionized water was replaced every 3 h.

2.1.4 Titration of NOSM with NO solution. The NOSM dispersion was titrated with an excess amount of saturated NO solution. NO stock solutions (1.8 mM, 25 °C) were prepared according to the reported method. NOSMs (2 mL, 0.1 g L^{-1}) were added into a standard cuvette (1 cm), and different amounts of the NO stock solution were added and incubated at room temperature for 30 s. The UV-vis spectra were then measured. A NO probe (5 μM) was used for fluorescence detection (λ_{ex} = 570 nm).

2.2 Cytotoxicity assay

Human bronchial epithelial cells (BESA-2B) and mouse mononuclear macrophages (Raw264.7) were cultured in a 96-well plate (2000 cells per well). After 24 h of incubation, the culture medium was replaced with 100 μL fresh medium containing NOSM micelles (0, 0.025, 0.05, and 0.1 mg mL^{-1}). After 24 h of incubation, 10 μL MTT reagent (5 mg mL^{-1} in PBS buffer) was added into each well and further incubated for 6 h. The medium was removed and replaced with 150 μL DMSO dissolving formazan for 20 min at room temperature. The absorbance values were recorded at a wavelength of 490 nm using a microplate reader (Thermo Fisher Scientific). The above experiment was repeated using Raw264.7 cells with the same method.

2.3 Live/dead staining assay

The safety of NOSMs in BESA-2B cells and Raw267.4 cells was further demonstrated by calcein AM/PI (Beyotime, Shanghai, China) staining assay. Both cells were seeded separately in 35 mm confocal dishes (10 000 cells per well) for 16 h, and then the NOSMs (0.1 mg mL^{-1}) were added to the medium. After 24 h, the medium was removed carefully and the cells were washed with 500 μL PBS. Calcein AM/PI probes were added to the well with final concentrations of 2.8 and 12 μM, respectively. The mixtures were incubated at 37 °C for 30 min, then washed three times with 500 μL PBS and imaged using a Leica SP5 confocal laser scanning microscope (CLSM).

2.4 Quantification of nitrite and proinflammatory cytokines in LPS-induced cells

RAW264.7 cells were seeded in a 24-well plate at a density of 20 000 cells per well After culturing for 24 h, cells were treated with PBS, LPS (1 μg mL^{-1}), L-NAME (1 mM), or NOSMs (0.1 mg mL^{-1}). All groups were supplemented with LPS (1 μg mL^{-1}) except the PBS group. RAW264.7 cells were further incubated for 24 h at 37 °C, and then the culture supernatants were collected. RAW264.7 cells without LPS treatment were used as the negative control. We detected the nitrite content in the cell culture media of RAW264.7 cells with Griess reagent. The collected medium was added 50 μL per well into a 96-well plate, then an equal volume of Griess reagent was added (50 μL A solution + 50 μL B solution). The plate was gently shaken for 10 min at 37 °C, and the absorbance at 550 nm was recorded. The nitrite levels were determined by comparing the values to a standard calibration curve (0–200 μM) obtained from sodium nitrite. Furthermore, for the quantification of IL-6 and IFN-γ levels in LPS-induced RAW264.7 cells, the collected medium was placed into 96-well plates, then the IL-6 ELISA kit (Ruixin, Quanzhou, China) and IFN-γ ELISA kit (Ruixin, Quanzhou, China) were used. The concentrations in each well were determined following the manufacturer's protocol.

2.5 Asthma model and treatment

Female Balb/c mice aged 6–7 weeks, with a body weight controlled at 18–20 grams (Henan Scibios Biotech Co., Ltd) were divided into 3 groups (Normal, OVA, and NOSM), 10 mice per group. The Normal group without OVA-induced was used as the negative control. Sensitization protocol: intraperitoneal injection of sensitizing solution at day 0, day 7, and day 14. Each mouse was injected with 200 μL of sensitizing solution containing OVA (allergens: 0.5 mg mL^{-1}) and $Al(OH)_3$ (10 mg mL^{-1}) in sterile PBS. Challenge protocol: nebulization from day 21 to day 34 (14 times in total). The nebulization device was connected to a transparent container, and 500 μL PBS was added to the nebulizer before the machine started. Then 5 mL OVA solution (10 mg mL^{-1} in sterile PBS) was added when the mist was visible, each time for 30 min, from day 21 to day 34 for a total of 14 days. During nebulization, mice showed clinical manifestations such as face scratching and sneezing, and the lung tissue exhibited infiltration of inflammatory cells such as eosinophils and mast cells. Treatment protocol: after the last challenge day, the Normal group and OVA group were nebulized with 5 mL PBS, while the NOSM group was nebulized with 5 mL NOSM (0.1 mg mL^{-1} in sterile PBS), once a day, from day 35 to day 39, for 30 minutes each time. Regarding animal care and experimental procedures, they were approved by the Animal Ethics and Use Committee of the First Affiliated Hospital of Anhui Medical University (Animal Ethics Number: LISC20211519).

2.6 Western blot analysis for SIRT6 protein expression

In *in vivo* experiments, the lungs of asthma mice with different treatments were collected and immediately snap-frozen in liquid nitrogen after the mice were sacrificed. Then lung tissues were homogenized after adding radioimmunoprecipitation assay (RIPA) buffer (Beyotime, Shanghai, China) 250 μL per 20 mg of tissue and serine protease inhibitor (PMSF) solution (Beyotime, Shanghai, China) (concentration of 1 mmol L^{-1}) on ice using steel balls. The mixture was centrifuged at 12 000*g* and 4 °C for 10 min to obtain the supernatant. Finally, 5× SDS-PAGE sample loading buffer (Beyotime, Shanghai, China) was added into a part of the supernatant, then the mixture was

denatured at 100 °C for 10 min and stored at −20 °C for further use.

Lysates were then loaded onto sodium dodecyl sulfate-polyacrylamide gel (SDS-PAGE) and the separated proteins were accurately transferred to polyvinylidene fluoride (PVDF) membranes (Millipore, Burlington, MA, USA). 5% skim milk was used to block at room temperature for 1 hour to ensure a clean experimental environment. The specific anti-SIRT6 (Proteintech Group, Wuhan, China) antibody (1 : 1000 dilution) was incubated with the target protein on the membrane at 4 °C overnight, followed by incubation with the enzyme-labeled secondary antibody (such as goat anti-rabbit IgG-HRP, 1 : 5000 dilution) at room temperature for 1 hour, forming a stable complex that was easy to detect. Finally, the membranes were imaged in a dark room.

2.7 Detection of nitrite and proinflammatory cytokine *in vivo*

Perform Western Blotting analysis on lung tissue by extracting the total protein from a portion of the lung tissue. The lysates were quantitated using a BCA Protein Assay Kit (Jiancheng, Nanjing, China). For blood analysis, whole blood was collected from mice in each group on the last day and then the serum was obtained *via* centrifugation at 1500 rpm for 20 min from whole blood. The nitrite content in lung tissue and serum was determined using Griess reagent (the method is the same as in section 2.5). The levels of inflammatory factors (IL-6, IL-13, and IFN-γ) were quantified using enzyme-linked immunosorbent assay (ELISA) kits (Ruixin, Quanzhou, China) according to the manufacturer's instructions.

2.8 Lung tissue pathological section

The tissue was washed multiple times with PBS and soaked in 4% paraformaldehyde at room temperature for 24 h. The fixed tissue was dehydrated and clarified, then embedded in paraffin at 60 °C and prepared into 4 μm slices. Then, according to the specific purpose of the experiment, periodic acid-Schiff (PAS) glycogen staining or Hematoxylin and Eosin (H&E) staining were performed on mouse tissue.

2.9 Statistical analysis

Data analysis was performed using GraphPad Prism 10 (GraphPad Software, USA) for statistical analysis. Treatment effects

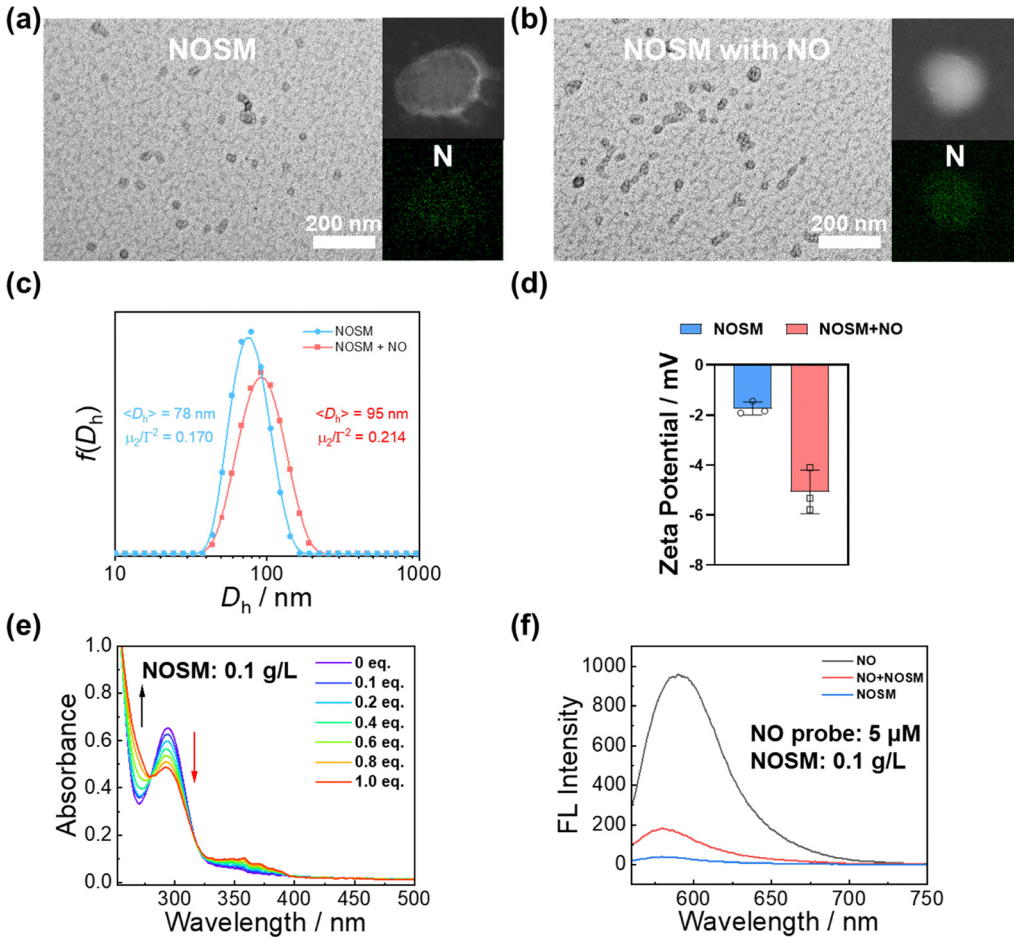

Fig. 1 Characterization of NOSMs. (a)–(c) TEM images and mapping and corresponding intensity-average hydrodynamic diameter distributions of aqueous dispersions of NOSMs and NOSMs with NO solution (phosphotungstic acid staining 2 wt%). (d) Zeta potentials of aqueous dispersions of NOSMs with or without NO solution. (e) UV/vis spectra of NOSM dispersion upon the addition of NO solution. (f) Fluorescence emission spectra (λ_{ex} = 570 nm) of the NO probe (5 μM) with NO solution, NOSMs (0.1 g L^{-1}) with NO solution, and NO probe and NOSMs (0.1 g L^{-1}) with NO probe.

were analyzed using one-way ANOVA, followed by Dunnett's multiple comparison test. WB quantitative detection was performed using the Image-G tool, with statistical analysis using $p < 0.05$ as the significance standard.

3. Results and discussion

3.1 Characterization of NOSMs

Endogenous gasotransmitter-responsive nanomaterials have attracted significant research attention.[30] Among these, *o*-phenylenediamine (*o*PDA) derivatives stand out as highly effective reactive molecules for NO, enabling the design of various NO-scavenging materials.[31] In this study, we developed a NO-scavenging platform capable of eliminating excess NO at lesion sites (Scheme 1). The micellar nanoparticles were constructed with NO-reactive *o*PDA derivatives within the cores, which effectively reduce NO levels through the formation of benzotriazole (BTA) moieties. The diblock copolymer was synthesized *via* reversible addition–fragmentation chain-transfer (RAFT) polymerization.[32] The chemical structure of the synthesized block copolymer was verified using NMR spectroscopy and size-exclusion chromatography (Fig. S2, ESI†).

As shown in Fig. 1a–c, the diblock copolymer self-assembled into NOSMs with an average hydrodynamic diameter, $\langle D_h \rangle$, of 78 nm. After reacting with a saturated NO solution, the

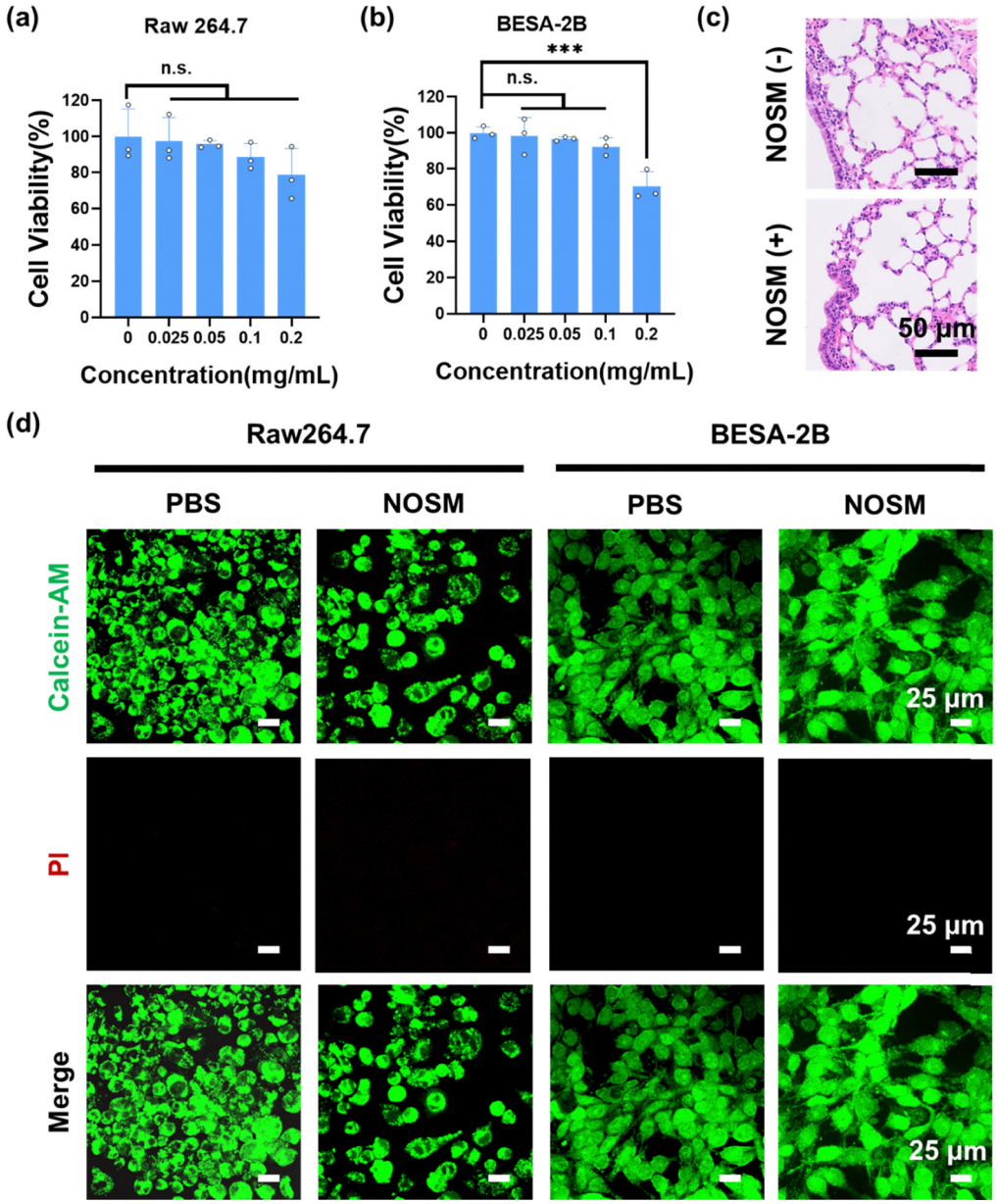

Fig. 2 The safety of NOSMs (a) and (b) MTT analysis of Raw264.7 and BESA-2B cells incubated with different concentrations of NOSM samples (n = 3). (c) Healthy Balb/c mice inhaled NOSM nebulization, and lung tissue harvested for HE staining. (d) Live/dead staining assay of NOSMs in Raw264.7 and BESA-2B cells, scale bar 25 μm.

nanoparticle size increased slightly, while elemental mapping revealed a significant rise in N content post-reaction. When stored at 37 °C for 7 days or under varying pH conditions, the particle size remained stable, demonstrating that the micelles possess excellent stability (Fig. 1a–c, and Fig. S3, ESI†). Zeta potential measurements revealed that the nanoparticles carried a negative charge both before and after the reaction (−1.7 mV and −5.1 mV) (Fig. 1d).[33,34] The zeta potential of the NOSM was found to be approximately −1.7 mV. Additionally, after the NOSM reacted with NO, the zeta potential slightly decreased to −5.1 mV (Fig. 1d). However, we observed a continuous decrease in absorbance centered at 294 nm (Fig. 1e). The NO-scavenging capability of NOSMs was further validated through fluorescence testing. The pyronine-based NO probe was selectively activated by NO.[35] After the addition of the NO probe following the reaction of the NO solution with the scavenging micelles, a significant decrease in fluorescence intensity was observed (Fig. 1f). Through these monitoring methods, the NO-scavenging properties of NOSM were confirmed.

3.2 Safety of NOSMs *in vitro*

By comparing the MTT experimental results of Fig. 2a and b, we observed that NOSM concentrations ranging from 0 to 0.1 g L^{-1} exhibited no cytotoxicity toward RAW264.7 and BESA-2B cells. However, when the concentration increased to 0.2 g L^{-1}, the cell viability of BSA cells decreased to 70%. However, the NO-scavenging efficiency of NOSMs improved with increasing concentration (Fig. S4, ESI†). Balancing the NO-scavenging efficiency and cytotoxicity, we selected 0.1 g L^{-1} NOSMs for subsequent experiments. From the results of the calcein-AM/PI staining technique, all cells were stained green with AM (acetoxymethyl ester of calcein), while dead cells were identified by red fluorescence from propidium iodide (PI) staining. It is noteworthy that no significant red fluorescence was observed in the cell staining, indicating that the cells remained viable. This also demonstrates that NOSMs (0.1 g L^{-1}) are biocompatible and non-toxic materials (Fig. 2d).[36] In addition, it can be found that there is no significant impact on the inflammatory cells and airway structure of the mouse lung tissue when NOSMs nebulized into the airway of mice (Fig. 2c).

3.3 *In vitro* anti-inflammatory evaluation of NOSMs

We next constructed a model of LPS-induced macrophage inflammation. Upon the addition of LPS, M0 cells differentiate into M1 cells. PBS, NOSMs, and L-NAME were added to the culture medium. Nitrite, IL-6, and INF-γ were tested to evaluate the anti-inflammatory efficacy of NOSMs (Fig. 3a). Compared to the PBS control group, the NO concentration in the LPS group significantly increased, showing a clear statistical difference.

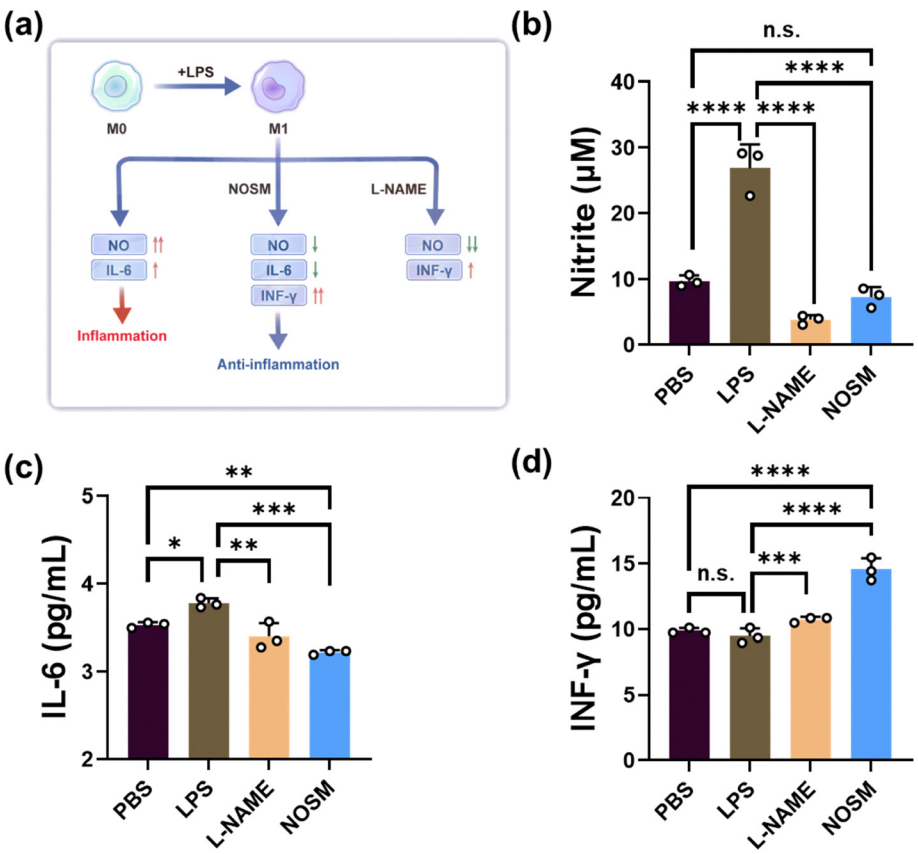

Fig. 3 NOSMs effectively clear NO *in vitro*, inhibit the release of IL-6, and increase the concentration of IFN-γ. (a) Raw264.7 cells were treated with PBS, LPS (1 μg mL^{-1}), L-NAME (1 mmol), or NOSMs (0.1 mg mL^{-1}). (b)–(d) The nitrite IL-6 and IFN-γ levels analysis after treatment with LPS, L-NAME, and NOSMs.

Conversely, the NO concentration in the NOSM group did not show a significant increase, compared to the LPS group. Similarly, the NO concentration in the L-NAME group was significantly reduced, also exhibiting statistical significance compared to the PBS control group. Therefore, it can be inferred that NOSMs have a good effect in clearing NO. As we all know, high concentrations of NO may participate in the occurrence, development, and airway structural remodeling of asthma through multiple pathways such as NO-cGMP-PKG-TRPVl, NO-cGMP-PKG-MAPK, and NO-cAMP-PKA-CREB.[15,22,23] A meta-analysis by Pan *et al.* further indicated that serum IL-6 levels in asthmatic patients were significantly higher than those in healthy non-asthmatic individuals, highlighting IL-6 as an important auxiliary marker for distinguishing between these two groups.[36] It can be inferred that NOSMs reduce IL-6 production by macrophages, suggesting their potential therapeutic value in the treatment of asthma. As shown in Fig. 3c, in addition to nitric oxide, LPS-induced inflammatory responses in macrophages led to a significant increase in intracellular cytokines, such as IL-6. In contrast, NOSMs can significantly inhibit IL-6 levels, suggesting that NOSMs inhibit IL-6 by reducing NO. In addition, IFN-γ as a potential therapeutic target, warrants further exploration for its application in asthma treatment.[37] In further comparison with the PBS control group, we observed that the IFN-γ concentrations in both the LPS group and the L-NAME group did not show significant

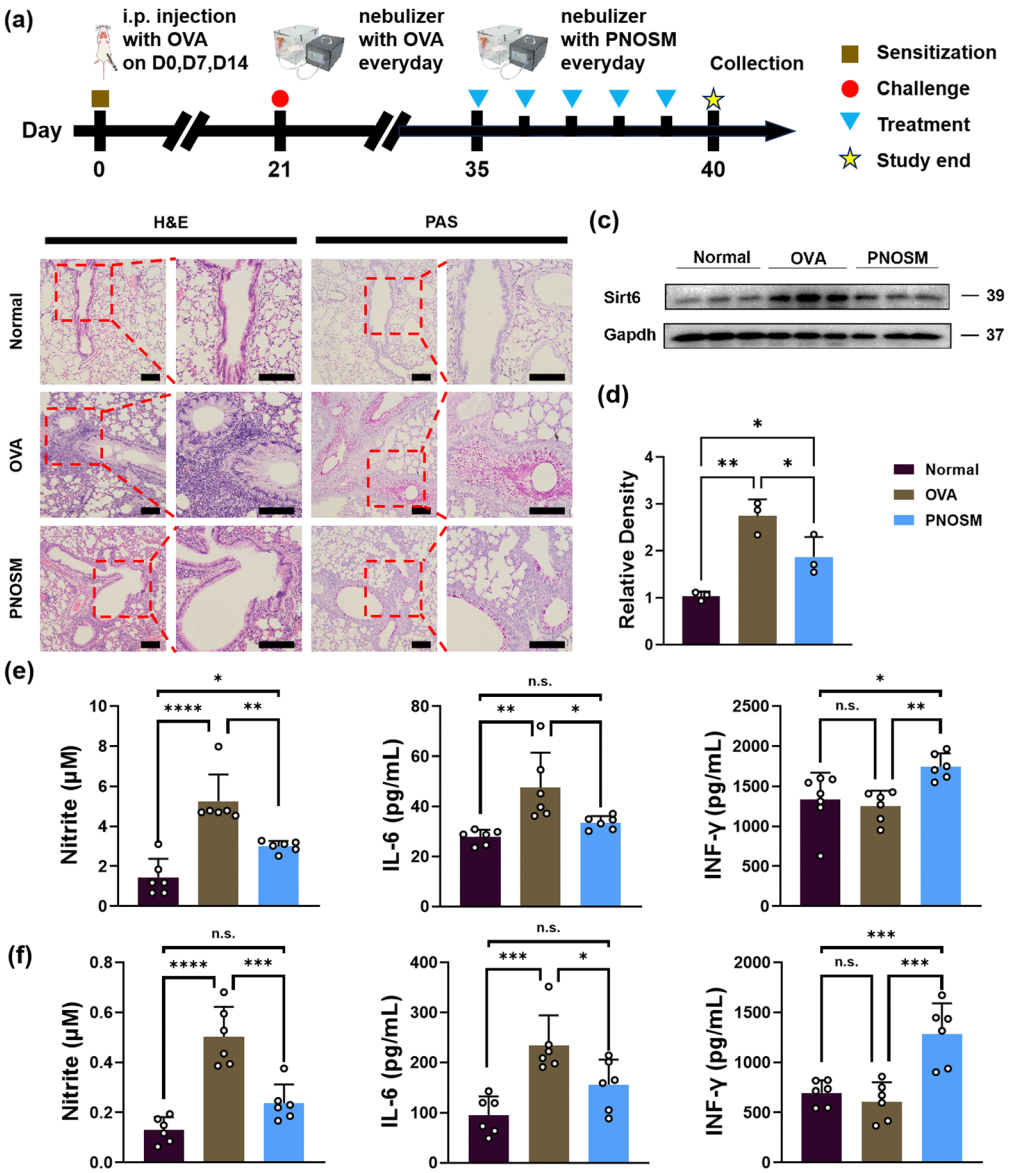

Fig. 4 (a) Timeline: sensitization: i.p. injection with 200 μL of sensitizing solution containing OVA and $Al(OH)_3$ in sterile PBS on day 0, 7, and 14; challenge: with OVA (10 mg mL^{-1}) nebulizer day 21 to day 34; treatment: 5 mL NOSM (0.1 mg mL^{-1}), once a day, day 35 to day 39. (b) The typical picture of H&E and PAS, scale bar 100 μm. (c) and (d) SIRT6 levels of WB and ImageJ analysis after treatment with OVA and NOSM. (e) and (f) IL-6, NO, and IFN-γ concentrations in lung tissues and blood (n = 6).

fluctuations. However, it is noteworthy that the IFN-γ concentration in the NOSM group showed a clear upward trend compared to the PBS control group (Fig. 3d). Therefore, NOSMs significantly enhance the ability of macrophages to produce IFN-γ, thereby strengthening its role in immune regulation.

In this experiment, we observed that high concentrations of NO inhibit the secretion of IFN-γ, which is primarily derived from Th1 cells. This further indicates that NO can suppress the activity of Th1 cells.[38–40] Through animal experiments on mice, we found that NOSMs significantly reduced NO levels in plasma and lung tissue, which in turn inhibited the production of IL-13 and promoted the production of IFN-γ.

3.4 NOSM treatment of mouse allergic asthma

The construction and treatment of asthmatic mice are shown in Fig. 4a. The mice were randomly divided into three groups (10 mice per group), including PBS, OVA, and NOSM (0.1 mg mL^{-1}). After the last challenge day, the Normal group and OVA group were nebulized with PBS, while the NOSM group was nebulized with NOSMs, once a day, from day 35 to day 39 for 30 minutes each time. Finally, on day 40, eyeball blood was collected, mice were euthanized, and tissue samples were preserved.

From the HE staining results, the number of inflammatory cells (including neutrophils, mast cells, and eosinophils) in the OVA group was significantly increased, and the bronchial mucosal folds showed obvious elongation and thickening, with some lumens narrowing to a much greater extent than in the normal and NOSM treatment groups (Fig. 4b). From the PAS staining results, the number of goblet cells and the amount of mucus secreted in the OVA group were significantly higher compared to those of the normal and NOSM groups. The NOSM group also showed an increase in goblet cells and mucus secretion. These pathological findings support the airway hyperresponsiveness and chronic inflammation associated with allergic asthma, leading to excessive mucus secretion. After NOSM treatment, the goblet cells and mucus glands in the mouse lung tissue and their secretion improved (Fig. 4b). Therefore, NOSMs effectively cleared NO from the airways, significantly alleviated airway inflammation, and improved airway remodeling.

As an important histone deacetylase involved in epigenetic regulation, SIRT6 is a convergence point for stress signaling pathways and transcriptional regulation, playing a crucial role in maintaining cellular homeostasis. Current research on SIRT6 in asthma indicates that SIRT6 is closely related to the occurrence of asthma and airway remodeling, and reducing SIRT6 can improve the clinical manifestations of OVA-sensitized asthmatic mice.[41–43] Research by Professor Lai Tianwen's team revealed the potential of targeting SIRT6 inhibition in reducing airway inflammation and remodeling in mice.[44] Herein, we subsequently conducted western blot (WB) experiments to examine changes in SIRT6 expression in lung tissues. The SIRT6 protein level in the OVA group was significantly higher than that in the control and treatment groups (Fig. 4c and d, and Fig. S5, ESI†).

Additionally, we assessed the levels of inflammatory factors in serum and lung tissue to evaluate the *in vivo* anti-inflammatory effects of NOSMs. We compared the concentrations of IL-6, IL-13, nitrite, and IFN-γ in lung tissues and blood. The results in Fig. 4e and f indicate that IL-6, IL-13, and nitrite concentrations were significantly elevated in the OVA group compared to the NOSM and normal groups. No significant differences were observed in the levels of IL-6, IL-13, and NO between the NOSM and normal groups. In contrast, the IFN-γ concentration with NOSM nebulization was significantly higher than that in both the OVA and normal groups. Therefore, we demonstrated that NOSMs could efficiently reduce the level of SIRT6 and alleviate airway inflammation, cytokine release, and mucus secretion in asthmatic mice through scavenging NO. Fortunately, throughout the entire treatment period, none of the mice experienced unusual weight fluctuations, and no noticeable liver toxicity or organ damage was detected (Fig. S7, ESI†), demonstrating the outstanding biocompatibility and safety of NOSM in living organisms.

4. Conclusion

In summary, our research demonstrated that NOSMs not only possess non-toxic and safe characteristics but also exhibit significant NO clearance capabilities. In *in vitro* experiments, the anti-inflammatory effects of NOSMs were further validated by reducing NO levels. Building on this foundation, we systematically evaluated the efficacy and safety of NOSMs in treating allergic asthma mice sensitized and challenged with OVA. Through *in vivo* treatment experiments, we found that NOSMs effectively reduced airway NO concentration and SIRT6 levels, significantly inhibiting inflammatory responses and the release of inflammatory factors. Therefore, our research indicated that NOSMs hold great potential and broad prospects as a candidate drug for treating allergic asthma-related airway inflammation.

Author contributions

Ding Shenggang: conceptualization, methodology, data management, investigation, formal analysis, writing—original draft, visualization, review, and editing. Rong Daoxiang and Fang Shanshan: conceptualization, methodology, investigation, data management, formal analysis, and writing—review, and editing. Huo Shaohu: methodology, investigation, and data management. Lin Paiyan: methodology and investigation. Cheng Jian: methodology and investigation. Hong Jingfang: methodology and investigation. Ding Shenggang and Rong Daoxiang: review and editing, resources, and funding acquisition. Cheng Jian, Hong Jingfang: review and editing, and project management. Ding Shenggang and Rong Daoxiang: project management, supervision, resources, and writing—review and editing.

Data availability

The data used to support the findings of this study are available from the corresponding author upon request.

Conflicts of interest

The authors declare that they have no known competing financial interests or personal relationships that could have influenced the work reported in this paper.

Acknowledgements

This work was funded by the Anhui Province Health Research Youth Project (AHWJ2023A30008) and the National Natural Science Foundation of China project (no. 52273113 and no. 22305239).

References

1 M. Sockrider and L. Fussner, What is asthma?, *Am. J. Respir. Crit. Care Med.*, 2020, **202**(1), P25–P26, DOI: **10.1164/rccm.202001-0001SO**.
2 B. J. Mathis, M. Kusumoto, A. Zaboronok and Y. Hiramatsu, Packaging and delivery of asthma therapeutics, *Pharmaceutics*, 2021, **14**(1), 92, DOI: **10.3390/pharmaceutics14010092**.
3 R. Pawankar, Allergic diseases and asthma: A global public health concern and a call to action, *World Allergy Organ. J.*, 2014, **7**(1), 12, DOI: **10.1186/1939-4551-7-12**.
4 A. Ahmad, Pharmacological strategies and recent advancement in nano-drug delivery for targeting asthma, *Life*, 2022, **12**(5), 596, DOI: **10.3390/life12050596**.
5 R. Newton and M. A. Giembycz, Understanding how long-acting β(2) -adrenoceptor agonists enhance the clinical efficacy of inhaled corticosteroids in asthma—An update, *Br. J. Pharmacol.*, 2016, **173**(19), 3405–3430, DOI: **10.1111/bph.13470**.
6 R. Newton, Anti-inflammatory glucocorticoids: Changing concepts, *Eur. J. Pharmacol.*, 2014, **724**, 231–236, DOI: **10.1016/j.ejphar.2013.12.006**.
7 L. M. Sevilla, A. Jiménez-Panizo, A. Alegre-Martí, E. Estébanez-Perpiñá, C. Caelles and P. Pérez, Glucocorticoid resistance: Interference between the glucocorticoid receptor and the MAPK signalling pathways, *Int. J. Mol. Sci.*, 2021, **22**(19), 10049, DOI: **10.3390/ijms221910049**.
8 S. C. Lin, L. S. Shi and Y. L. Ye, Advanced molecular knowledge of therapeutic drugs and natural products focusing on inflammatory cytokines in asthma, *Cells*, 2019, **8**(7), 685, DOI: **10.3390/cells8070685**.
9 J. B. Rice, A. G. White, L. M. Scarpati, G. Wan and W. W. Nelson, Long-term systemic corticosteroid exposure: A systematic literature review, *Clin. Ther.*, 2017, **39**(10), 2216–2229, DOI: **10.1016/j.clinthera.2017.08.008**.
10 R. Aalbers, C. Vogelmeier and P. Kuna, Achieving asthma control with ICS/LABA: A review of strategies for asthma management and prevention, *Respir. Med.*, 2016, **111**, 1–7, DOI: **10.1016/j.rmed.2016.01.001**.
11 P. J. Barnes, Theophylline, *Am. J. Respir. Crit. Care Med.*, 2013, **188**(8), 901–906, DOI: **10.1164/rccm.201304-0763CI**.
12 S. G. Wendell, H. Fan and C. Zhang, G Protein-coupled receptors in asthma therapy: Pharmacology and drug action, *Pharmacol. Rev.*, 2020, **72**(1), 1–49, DOI: **10.1124/pr.119.018267**.
13 M. Harada, T. Hirota, A. I. Jodo, Y. Hitomi, M. Sakashita, T. Tsunoda, T. Miyagawa, S. Doi, M. Kameda and K. Fujita, *et al.*, Thymic stromal lymphopoietin gene promoter polymorphisms are associated with susceptibility to bronchial asthma, *Am. J. Respir. Cell Mol. Biol.*, 2011, **44**(6), 787–793, DOI: **10.1165/rcmb.2010-0223OC**.
14 A. Jo-Watanabe, T. Okuno and T. Yokomizo, The role of leukotrienes as potential therapeutic targets in allergic disorders, *Int. J. Mol. Sci.*, 2019, **20**(15), 3580, DOI: **10.3390/ijms20153580**.
15 T. Yokomizo, M. Nakamura and T. Shimizu, Leukotriene receptors as potential therapeutic targets, *J. Clin. Invest.*, 2018, **128**(7), 2691–2701, DOI: **10.1172/JCI97729**.
16 N. Habib, M. A. Pasha and D. D. Tang, Current understanding of asthma pathogenesis and biomarkers?, *Cells*, 2022, **11**(17), 2764, DOI: **10.3390/cells11172764**.
17 A. Manda-Handzlik, W. Bystrzycka and A. Cieloch, *et al.*, Nitric oxide and peroxynitrite trigger and enhance release of neutrophil extracellular traps, *Cell. Mol. Life Sci.*, 2020, **77**(5663), 1–17, DOI: **10.1007/s00018-019-03331-x**.
18 C. Klose, The neuropeptide neuromedin U stimulates innate lymphoid cells and type 2 inflammation, *Nature*, 2017, **549**(7671), 282–286, DOI: **10.1038/nature23676**.
19 F. Ding, B. Liu and W. Zou, *et al.*, LPS exposure in early life protects against mucus hypersecretion in Ovalbumin-Induced asthma by down-regulation of the IL-13 and JAK-STAT6 pathways, *Cell. Physiol. Biochem.*, 2018, **46**(3), 1263–1274, DOI: **10.1159/000489239**.
20 X. Zhou, H. Hu and S. Balzar, *et al.*, MAPK regulation of IL-4/IL-13 receptors contributes to the synergistic increase in CCL11/eotaxin-1 in response to TGF-β1 and IL-13 in human airway fibroblasts, *J. Immunol.*, 2012, **188**(12), 6046–6054, DOI: **10.4049/jimmunol.1102760**.
21 K. Asosingh, C. D. Lauruschkat and M. Alemagno, *et al.*, Arginine metabolic control of airway inflammation, *JCI Insight*, 2020, **5**(2), e127801, DOI: **10.1172/jci.insight.127801**.
22 R. A. Dweik, S. A. Comhair and B. Gaston, *et al.*, NO chemical events in the human airway during the immediate and late antigen-induced asthmatic response, *Proc. Natl. Acad. Sci. U. S. A.*, 2001, **98**(5), 2622–2627, DOI: **10.1073/pnas.051629498**.
23 J. G. Kim, M. J. Kim and J. S. Lee, *et al.*, Smilax guianensis Vitman Extract Prevents LPS-Induced Inflammation by Inhibiting the NF-kB Pathway in RAW 264.7 Cells, *J. Microbiol. Biotechnol.*, 2020, **30**(6), 822–829, DOI: **10.4014/jmb.2003.03012**.
24 D. P. Green, N. Limjunyawong and N. Gour, *et al.*, A Mast-Cell-Specific Receptor Mediates Neurogenic Inflammation and Pain, *Neuron*, 2019, **101**(3), 412–420, DOI: **10.1016/j.neuron.2019.01.003**.
25 S. Lea, J. Li and J. Plumb, *et al.*, P38 MAPK and glucocorticoid receptor crosstalk in bronchial epithelial cells, *J. Mol. Med.*, 2020, **98**(3), 361–374, DOI: **10.1007/s00109-019-01847-2**.
26 G. Leyva-Gómez, H. Cortés, J. J. Magaña, N. Leyva-García, D. Quintanar-Guerrero and B. Florán, Nanoparticle

technology for treatment of Parkinson's disease: The role of surface phenomena in reaching the brain, *Drug Discovery Today*, 2015, **20**(7), 824–837, DOI: 10.1016/j.drudis.2015.03.010.

27 W. Yang, Z. Dong, Y. Li, Y. Zhang, H. Fu and Y. Xie, Therapeutic efficacy of chitosan nanoparticles loaded with BCG-polysaccharide nucleic acid and ovalbumin on airway inflammation in asthmatic mice, *Eur. J. Clin. Microbiol. Infect. Dis.*, 2021, **40**(8), 1623–1631, DOI: 10.1007/s10096-021-04160-1.

28 Y. Lv, J. Zhang and C. Wang, Self-assembled chitosan nanoparticles for intranasal delivery of recombinant protein interleukin-17 receptor C (IL-17RC): Preparation and evaluation in asthma mice, *Bioengineered*, 2021, **12**(1), 3029–3039, DOI: 10.1080/21655979.2021.1926218.

29 D. Zhao, D. Li, X. Cheng, Z. Zou, X. Chen and C. He, Mucoadhesive, antibacterial, and reductive nanogels as a mucolytic agent for efficient nebulized therapy to combat allergic asthma, *ACS Nano*, 2022, **16**(8), 11161–11173, DOI: 10.1021/acsnano.2c03202.

30 S. Tao, J. Cheng, G. Su, D. Li, Z. Shen, F. Tao, T. You and J. Hu, Breathing Micelles for Combinatorial Treatment of Rheumatoid Arthritis, *Angew. Chem., Int. Ed.*, 2020, **59**(49), 21864–21869, DOI: 10.1002/anie.202010009Epub 2020 Oct 13. PMID: 32902083.

31 J. Hu, M. R. Whittaker, H. Duong, Y. Li, C. Boyer and T. P. Davis, Biomimetic polymers responsive to a biological signaling molecule: Nitric oxide (NO) triggered reversible self-assembly of single macromolecular chains into nanoparticles, *J. Controlled Release*, 2015, **213**, e55–e56, DOI: 10.1016/j.jconrel.2015.05.091Epub 2015 Aug 19. PMID: 27005189.

32 C. Amgoth, G. Dharmapuri and A. M. Kalle, *et al.*, Nanoporous capsules of block co-polymers of [(MeO-PEG-NH)-*b*-(L-GluA)]-PCL for the controlled release of anticancer drugs for therapeutic applications, *Nanotechnology*, 2016, **27**(12), 125101, DOI: 10.1088/0957-4484/27/12/125101.

33 Chander Amgoth, D. S. Doddapaneni Suman Joshi and Gangappa Dharmapuri, *et al.*, Self-assembled block copolymer [(BenzA)-*b*-(PCL)] micelles to orient randomly distributed AuNPs into hollow core-shell morphology and its role as payload for nanomedicines, *Mater. Sci. Eng., C*, 2018, **92**, 790–799, DOI: 10.1016/j.msec.2018.07.033.

34 C. Amgoth and S. Joshi, Thermosensitive block copolymer [(PNIPAM)-*b*-(Glycine)] thin film as protective layer for drug loaded mesoporous silica nanoparticles, *Mater. Res. Express*, 2017, **4**(10), 105306, DOI: 10.1088/2053-1591/aa91eb.

35 H. Zheng, G. Q. Shang, S. Y. Yang, X. Gao and J. G. Xu, Fluorogenic and chromogenic rhodamine spirolactam based probe for nitric oxide by spiro ring opening reaction, *Org. Lett.*, 2008, **10**(12), 2357–2360, DOI: 10.1021/ol800206x Epub 2008 May 17. PMID: 18484726.

36 R. Pan, S. Kuai and Q. Li, *et al.*, Diagnostic value of IL-6 for patients with asthma: A meta-analysis, *Allergy, Asthma, Clin. Immunol.*, 2023, **19**(1), 39, DOI: 10.1186/s13223-023-00794-3.

37 R. K. Kumar, D. C. Webb and C. Herbert, *et al.*, Interferon-gamma as a possible target in chronic asthma, *Inflammation Allergy: Drug Targets*, 2006, **5**(4), 253–256, DOI: 10.2174/187152806779010909.

38 C. Bogdan, Nitric oxide and the immune response, *Nat. Immunol.*, 2001, **2**, 907–916.

39 J. D. MacMicking, C. Nathan, G. Hom, N. Chartrain, D. S. Fletcher and M. Trumbauer, *et al.*, Altered responses to bacterial infection and endotoxic shock in mice lacking inducible nitric oxide synthase, *Cell*, 1995, **81**, 641–650.

40 X. Q. Wei, I. G. Charles, A. Smith, J. Ure, G. J. Feng and F. P. Huang, *et al.*, Altered immune responses in mice lacking inducible nitric oxide synthase, *Nature*, 1995, **375**, 408–411.

41 K. Asosingh, C. D. Lauruschkat and M. Alemagno, *et al.*, Arginine metabolic control of airway inflammation, *JCI Insight*, 2020, **5**(2), e127801, DOI: 10.1172/jci.insight.127801.

42 H. Y. Jang, S. Gu, S. M. Lee and B. H. Park, Overexpression of sirtuin 6 suppresses allergic airway inflammation through deacetylation of GATA3, *J. Allergy Clin. Immunol.*, 2016, **138**(5), 1452–1455, DOI: 10.1016/j.jaci.2016.05.019.

43 F. Liu and Y. X. Shang, Sirtuin 6 attenuates epithelial–mesenchymal transition by suppressing the TGF-β1/Smad3 pathway and c-Jun in asthma models, *Int. Immunopharmacol.*, 2020, **82**(February), 106333, DOI: 10.1016/j.intimp.2020.106333.

44 J. Quan, X. Wen and G. Su, *et al.*, Epithelial SIRT6 governs IL-17A pathogenicity and drives allergic airway inflammation and remodeling, *Nat. Commun.*, 2023, **14**(1), 8525.